

Poly(dimethyltin glutarate) as a Prospective Material for High Dielectric Applications

Aaron F. Baldwin, Rui Ma, Arun Mannodi-Kanakkithodi, Tran Doan Huan, Chenchen Wang, Matthew Tefferi, Jolanta E. Marszalek, Mukerrem Cakmak, Yang Cao, Rampi Ramprasad, and Gregory A. Sotzing*

The ability of atoms within a material to spontaneously orient themselves from their equilibrium positions with respect to an applied electric field make them ideal for a number of applications, including photovoltaics, transistors, and capacitors, in which a dielectric is required.^[1] The role of these applications is growing exponentially, as a result of their ability to store, convert, or amplify power, thus making the need for new dielectric materials more critical. Ideally, the development of universal dielectric materials that can either fulfill multiple needs within a subset of one application or across a full spectrum would be accomplished. To achieve this, high-dielectric-constant materials are required especially to allow for continual device miniaturization.

Polymers offer improved processing conditions and lower densities versus inorganic materials but exhibit lower dielectric constants. This is a result of the negligible contribution of the ionic component to the total dielectric constant.^[2] The ionic component can be enhanced by incorporation of permanent dipoles either in the backbone or as pendant groups but usually at a cost of reduced band gap. In fact, the limit in the total dielectric constant of many linear polymers is inversely proportional to their band gap.^[2,3] An exception to this is poly(vinylidene fluoride), PVDF, which has a band gap of 6 eV and a dielectric constant >10.^[4] However, it is a ferroelectric material and must be poled as it does not crystallize into a polar form.^[5] Copolymerization of VDF with other derivatives, such as hexafluoropropylene, trifluoroethylene, or chlorotrifluoroethylene, crystallize in polar forms and reduce the amount of

ferroelectricity but with lower dielectric constants as the copolymers formed are random in nature.^[5,6]

A second method to increase the permittivity of polymers is through the addition of high-dielectric-constant nanoparticles, such as barium titanate.^[7] However, an effective increase of the dielectric constant is not observed until a large volume of nanoparticles has been added to the matrix and it often faces the problem of agglomeration since it requires small particle sizes.^[7d] As a consequence of the large amount of nanoparticles present, the weight of the polymer film increases due to the higher density of the nanoparticle and the nanoparticle/polymer matrix can suffer from decreased electric breakdown strength.

Here, we consider the incorporation of metal atoms, such as tin, instead of nanoparticles into the polymer backbone as a means of enhancing the dielectric constant while still preserving low loss, since the metal atom is more polarizable than carbon. This approach, inspired by recent computation-guided findings that illustrate the benefits of incorporating a critical amount of tin in an organic polymer backbone, is expected to not lead to undesirable issues related to metal atom aggregation and/or dispersibility.^[8] Moreover, the amount of metal in the polymer can be controlled by the size of the organometallic monomers synthesized.

Polymers containing tin in the backbone are one of the more commonly studied organometallic polymers, with applications encompassing biocides, insecticides, fungicides, and antifouling agents.^[9] Carraher and co-workers have reported numerous tin-containing polymers with different tin-heteroatom bonds, while Stiegman and co-workers have reported a high-refractive-index thermoset material based on benzenedithiol and tetravinyltin.^[10] Here, we report the synthesis of a poly(organotin ester) based on dimethyltin dichloride and glutaric acid as a prospective dielectric material. Dimethyltin was utilized as the tin unit in the polymer in order to keep the free volume of the polymer chain as low as possible allowing for a larger dipolar and atomic polarizability within the polymer chain.^[11] The experimental dielectric measurements are strengthened with density functional theory (DFT) calculations to better explain the high dielectric constant through prediction of potential 3D organizations of this polymeric system. With organotin motifs suggested by high-throughput DFT computations, detailed structural models being predicted by DFT and subsequently confirmed with experimental measurements, the rational design of one subclass of dielectric materials is achieved.

The synthesis of poly(dimethyltin glutarate) (pDMTGlu) follows the interfacial polymerization described by Carraher and

Dr. A. F. Baldwin, R. Ma, Prof. G. A. Sotzing
Polymer Program
Institute of Materials Science
University of Connecticut
97 North Eagleville Rd, Storrs, Connecticut 06269, USA
E-mail: g.sotzing@uconn.edu

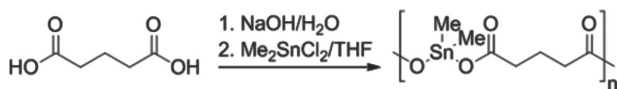
A. Mannodi-Kanakkithodi, Dr. T. D. Huan, C. C. Wang,
Prof. R. Ramprasad
Department of Materials Science and Engineering
Institute of Materials Science
University of Connecticut
97 North Eagleville Rd, Storrs, Connecticut 06269, USA

M. Tefferi, Prof. Y. Cao
Department of Electrical and Computer Engineering
University of Connecticut
97 North Eagleville Rd, Storrs, Connecticut 06269, USA

Dr. J. E. Marszalek, Prof. M. Cakmak
Department of Polymer Engineering
University of Akron
250 South Forge St, Akron, Ohio 44325, USA

DOI: 10.1002/adma.201404162





Scheme 1. Synthetic route to poly(dimethyltin glutarate).

co-workers with some modification (**Scheme 1**). The concentration of the tin monomer was increased in the organic phase and the organic phase was changed to a more polar solvent, tetrahydrofuran (THF) versus hexane, to increase the molecular weight of the polymer. The polymer exhibited solubility in both *m*-cresol and acetic acid. When dissolved in acetic acid, there was no evidence of methane evolution indicating that the polymer was stable in the acidic solution. A ^1H NMR sample was prepared under inert atmosphere with acetic acid- d_4 as solvent (see the Supporting Information). The spectra contained a triplet at $\delta = 2.46$ ppm (4H, CH_2), a quintet at $\delta = 1.94$ ppm (2H, CH_2), and a singlet at $\delta = 0.99$ ppm (6H, $\text{Sn}-\text{CH}_3$). Also present in the ^1H NMR spectrum were triplets at $\delta = 2.58$ ppm, a triplet at $\delta = 2.33$ ppm indicative of a butanoic acid chain end. From the integrations of the polymer and chain end peaks, the M_n was calculated to be $69\,000\text{ g mol}^{-1}$. The thermal properties of the polymer were measured by thermogravimetric analysis (TGA) and differential scanning calorimetry (DSC). The polymer exhibited thermal stability up to $235\text{ }^\circ\text{C}$ with a thermal transition at $119\text{ }^\circ\text{C}$ indicative of a melting/crystallization not related to a full phase transition of the polymer (see the Supporting Information). The thermal stability of pDMTGLu is well above that of most organic polymers used as dielectric materials in capacitors but below some high k polyimides previously reported.^[12] For example, good thermal stability is of significance for the reduction in the size of the cooling unit of the capacitor bank and an increase in the repetition rate of the capacitor.

The detailed atomic-level structures of pDMTGLu were determined using the DFT as implemented in the Vienna ab initio simulation package.^[13,14] The exchange–correlation interactions were treated within the semilocal Perdew, Burke, and Ernzerhof

(PBE) approximation.^[15] Starting from several random initial configurations of $-\text{COO}-\text{Sn}(\text{CH}_3)_2-\text{OOC}-(\text{CH}_2)_3-$, the repeating unit of the synthesized pDMTGLu, the possible low-energy structures were explored by the minima-hopping method.^[16] The dielectric constants of the predicted structures were then calculated within the density functional perturbation theory.^[17] Because conventional DFT calculations with PBE significantly underestimate the band gap, the HSE06 hybrid functional was used to better determine this quantity.^[18] The intermolecular van der Waals interactions, which play an essential role in stabilizing polymers, were estimated by DFT-D2, the method proposed by Grimme.^[19]

Four structural models of pDMTGLu, labeled as S1, S2, S3, and S4, were theoretically predicted to be lowest in energy and are illustrated in **Figure 1**. In all these structures, the Sn atoms are octahedral coordinated with nearest neighbors being two carbon atoms (part of two methyl groups) and four oxygen atoms (each pair part of the two adjacent COO carboxylate groups). Such complexes are linked together by three methylene (CH_2) groups. In S3 and S4, the two most stable structures, four Sn–O bonds link the central Sn atom with four O atoms from two carboxylate groups in the same repeating unit, thus realizing the hypothesized intrachain motif. The interchain motif is clearly shown in S1, of which two Sn–O bonds are used to link the chains together. Interestingly, the simulations predict that hybridization between the interchain and the intrachain motifs is also possible. In S2, for instance, these motifs are simultaneously observed. The intrachain motif is realized when the first carboxylate group is connected to the Sn atom by two Sn–O bonds. Of the two other Sn–O bonds, one links the central Sn atom with the second carboxylate group while the other interlinks chains, clearly leading to the interchain motif. Since these four structures are very close in energy, (see Figure 1), they may all coexist in the synthesized sample leading to properties that are averages of the four structures.

The theoretically predicted structural models are strongly supported by a very recent experiment. In particular, the intrachain

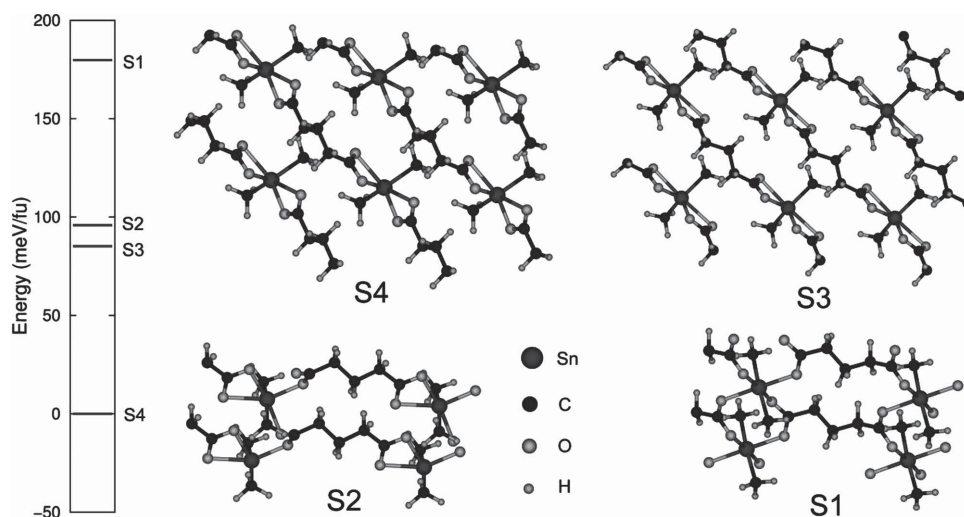


Figure 1. Geometries and energies of S1, S2, S3, and S4, the structures predicted for the Sn-based polymer with repeating unit $-\text{COO}-\text{Sn}(\text{CH}_3)_2-\text{OOC}-(\text{CH}_2)_3-$. Tin, carbon, oxygen, and hydrogen atoms are represented by dark blue-gray, burgundy, red, and pink spheres, respectively. The energy of these structures is given with respect to that of S4, the most stable predicted structure.

Table 1. Sn—O and Sn—C bond lengths (in Å) of S3 and S4 given in a comparison with those of Complex 4 and Complex 5 reported in ref. [20].

Bond	S3	Complex 5	S4	Complex 4
Sn—O1	2.174	2.113	2.114	2.140
Sn—O2	2.517	2.511	2.432	2.552
Sn—O3	2.171	2.113	3.098	>3
Sn—O4	2.553	2.511	2.105	2.136
Sn—C1	2.127	2.109	2.125	2.119
Sn—C2	2.126	2.109	2.132	2.130

motifs shown by S3 and S4 were observed in organotin carboxylates, the related crystals of which are also based on the —COO—Sn—OOC— unit.^[20] The Sn—O and Sn—C bond lengths of S3 and S4, as shown in Table 1, agree well with the corresponding bond lengths of Complex 5 and Complex 4, two experimentally determined structures of the organotin carboxylates (see the Supporting Information for positional details of the structures).^[20]

The formation of the Sn—O bond was confirmed by the shift of the carbonyl group of glutaric acid to a lower energy as seen in the IR (Figure 2). Carraher reports two absorption ranges for the carbonyl group in poly(tin carboxylates), 1635–1660 and 1550–1580 cm⁻¹ with pDMTGlu carbonyl absorptions at 1673 and 1563 cm⁻¹.^[21] Also indicative of the tin—oxygen bond formation is the combination of skeletal C—CO—O with Sn—O stretching at 645 cm⁻¹.^[21] It is well documented that tin mono- and dicarboxylates form coordination complexes.^[22] Peruzzo et al. hypothesized that both intra- and interchain complexes described above are present, with the bridging and nonbridging symmetric carbonyl bands exhibiting different absorptions, 1410–1430 and 1350–1370 cm⁻¹, respectively.^[23] The IR of pDMTGlu shows the formation of both complexes with absorptions at 1406 and 1378 cm⁻¹ (see the Supporting Information for fully labeled IR spectrum). The IR spectrum of the stabilized polymers was also calculated and the characteristic vibrational modes of the tin ester were identified. It is observed that the peaks in the IR intensity versus frequency plot obtained computationally match with the experimental IR peaks seen in

the transmittance versus frequency plot. Furthermore, the following observed stretching mode frequency matched with the frequency reported in Carraher's work: the C—CO—O stretching at 1294 cm⁻¹ (1250–1290 cm⁻¹). Figure 2 further illustrates the comparison of the experimental and computational IR spectra.

The dielectric constants ϵ , which are composed of an electronic component ϵ_{elec} and an ionic component ϵ_{ionic} , and the energy band gap E_g of the predicted structures were then determined. First, the refractive index of pDMTGlu was measured through ellipsometry on a film of the polymer, which had been spin-coated onto a silica wafer. The data were collected using reflection and fitted to a Cauchy model. From this fit, the refractive index of pDMTGlu was measured to be 1.59 at 632 nm. The relation of refractive index and ϵ_{elec} is by

$$n = \sqrt{\epsilon_{\text{elec}}} \quad (1)$$

The average ϵ_{elec} of the predicted structures is 2.716, which equates to a refractive index of 1.65. The reason for the slight difference in the measured and calculated refractive index could stem from some surface roughness of the polymer film, making the fit of the Cauchy model more difficult.

To compare the theoretical calculations to the experimental dielectric properties of pDMTGlu, a film of the polymer was solution casted from m-cresol onto a stainless steel shim stock. The film was air dried until tacky and further dried in vacuo for 24 h at 150 °C to drive off as much residual m-cresol as possible. The total thickness of film and shim stock is determined using a point-to-point measurement, in which the film thickness is determined by subtracting the thickness of the shim stock from the total. In order to test the dielectric properties, a silicone electrode is then placed on top of the dried film and compressed to ensure that air is absent between electrode and film. Table 2 shows a comparison of the theoretical results with the corresponding measured values. The dielectric constant ϵ of these stable 1D and 2D motifs are ranged from 3.9 to 5.5, with an averaged value, ϵ_{avg} , of 4.65. In contrast the ϵ_{avg} value, for five samples of pDMTGlu, over a frequency range of 1–10 000 Hz is 6.08 ± 1.90 , with specific values of each sample shown in Figure 3. The large standard deviation is most likely due to the nature of the film. Due to inability of precisely controlling the crystallization of this newly developed polymer, variations on morphology derived from different crystal sizes and

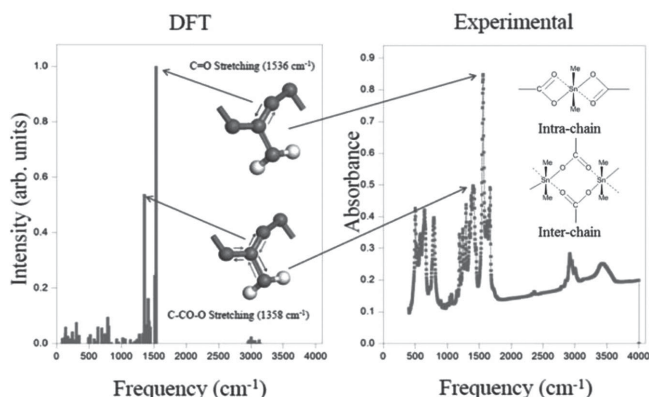


Figure 2. The C=O and C—CO—O stretching modes for S4, shown on the IR plots obtained from DFT results (left) as well as from experimental results (right).

Table 2. Dielectric constants ϵ , ϵ_{elec} , ϵ_{ionic} , and energy band gaps (E_g) calculated for the structural models S1, S2, S3, and S4 and measured values of poly(dimethyltin glutarate) (pDMTG) and biaxially oriented polypropylene (BOPP).

Structure	ϵ_{elec}	$\epsilon_{\text{ionic}}^a)$	ϵ_{total}	E_g [eV]
S1	2.832	2.608	5.439	5.731
S2	2.721	1.729	4.540	6.113
S3	2.664	2.179	4.842	6.361
S4	2.647	1.205	3.852	6.358
pDMTGlu	2.528 ^{b)}	3.692	$6.075 \pm 1.900^c)$	4.697
BOPP	2.220	0.260	2.480	7.000

^{a)} $\epsilon_{\text{ionic}} = \epsilon - \epsilon_{\text{elec}}$; ^{b)}Determined from RI; ^{c)}Averaged value, over a frequency range of 1–10 000 Hz, for five samples of pDMTGlu.

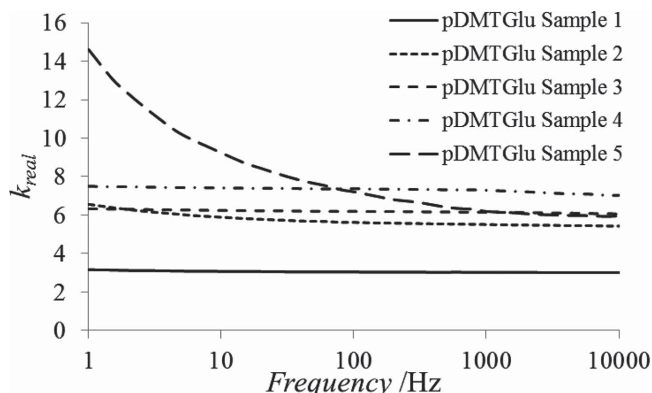


Figure 3. Dielectric constant for five samples of pDMTGlu.

amounts play important role on the dielectric properties. Large crystal size also brings problem on film processing, which was addressed here by polymer blending. The differences between experimental and theoretical values are a result of these inconsistencies as well as the calculations being run on highly crystalline systems at 0 K.

A film of pDMTGlu was solution cast from *m*-cresol onto a quartz slide and the UV absorbance measured to determine the energy band gap of the polymer. The energy band gap is calculated from Planck's relation

$$E_g = hc/\lambda_{\text{onset}} \quad (2)$$

From the UV data (see the Supporting Information), the onset occurs at 264 nm and the band gap is calculated to be 4.697 eV. The experimental band gap is approximately 24% lower than the averaged computed values of the four stable motifs. The reasoning for this difference in the values is that the calculations assume a fully crystalline material.

To confirm our hypothesis that the four stable predicted motifs are present in the sample in unequal amounts the predicted X-ray diffraction (XRD) pattern of the motifs and experimentally collected XRD of the polymer after precipitation from the reaction as well as after solubilizing and

recovery from *m*-cresol was compared (Figure 4). The initial polymer powder shows a conglomeration of all possible stable structures with rearrangement to one predominant crystal structure after dissolution in *m*-cresol which is signified by the disappearance of peaks in the XRD at 2θ values of 11.50 and 15.52. Comparison of the calculated and experimental XRD shows that the rearrangement of the crystal structure has the propensity to stabilize itself in the S4 configuration, since the S4 structure as well the polymer exhibit a peak at approximately a 2θ value of 15. This is also justified by the fact that the S4 crystal structure was calculated to be the lowest energy form.

As mentioned previously, the drawback of pDMTGlu is that it forms large crystals upon drying resulting in a very brittle film, which leads to a very low breakdown strength. To alleviate this, a second homopolymer (pDMTDMG), employing 3,3-dimethylglutaric acid (DMG) as a means of disrupting chain packing, was synthesized in the same manner as pDMTGlu (see the Supporting Information for synthetic details and characterization). A 20/80 (wt/wt) blend of both homopolymers, pDMTGlu and pDMTDMG, was mixed and dissolved in *m*-cresol at 5 wt% and drop-casted onto shim stocks and annealed at elevated temperature to drive off *m*-cresol. After the film dried to a point in which it was tacky, it was further dried in vacuo at 150 °C for 24 h. The dried film was clear with very small crystals not visible to the naked eye and better adhesion to the substrate. The surface roughness of the film was determined using mechanical profilometry and was measured between 12 and 28 nm, which is based on the 15- μm -thick sample, equate to a surface roughness of less than 1%. A silicone electrode was placed on top of film, still adhered to the shim stock, in order to test the dielectric properties. Figure 5 illustrates the frequency domain dielectric properties, in which the film has an average dielectric constant of 4.84 with dissipation less than 5% over the frequency range of 20–10⁶ Hz.

As a result of the small crystal size and better adhesion of the polymer blend versus just pDMTGlu, charge–discharge behavior of the blend was determined through D–E hysteresis loops (Figure 5), in which 0.07 cm² Au/Pd (80/20 wt%) electrodes are sputtered on top of the film. The blend was

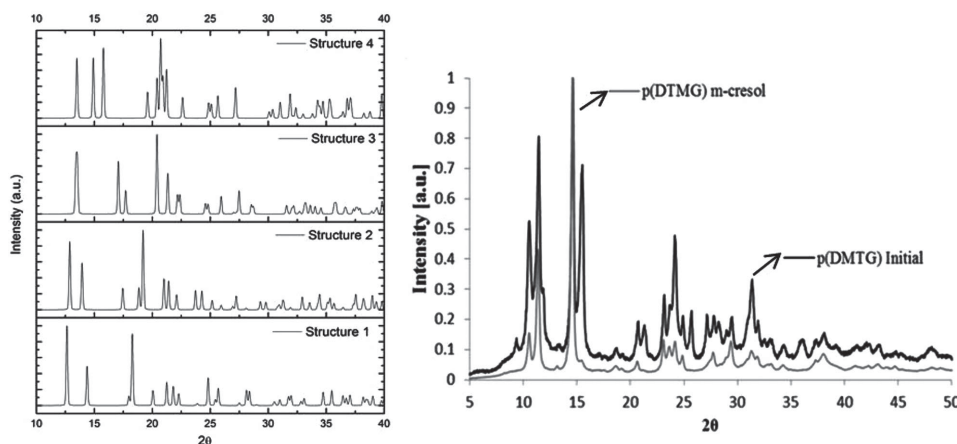


Figure 4. Predicted X-ray diffraction pattern (XRD) of the four stable motifs (left) and experimental XRD pattern of precipitated polymer and after solubilizing and recovering from *m*-cresol (right).

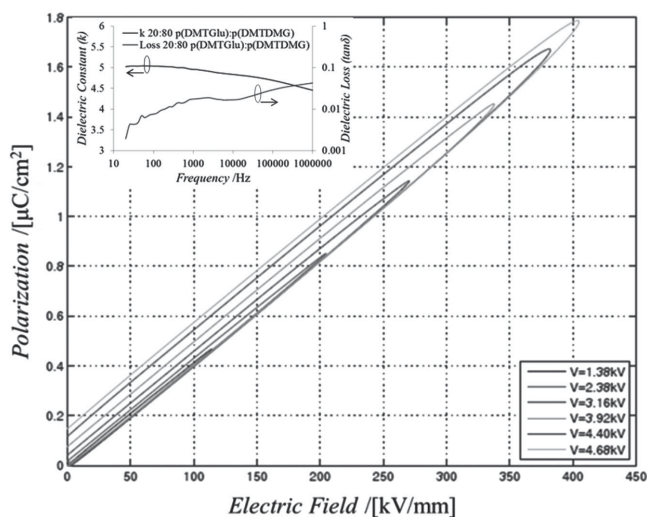


Figure 5. Frequency domain dielectric properties (inset) and polarization versus electric field loops for the 20/80 (wt/wt) blend of pDMTGlU/pDMTDMG, suggesting linear polarizations for electric fields up to 400 kV cm⁻¹. Dielectric permittivity derived from the DE loops is in agreement with frequency domain data over the range of 10–10⁶ Hz.

able to achieve stability of 380 ± 38 kV mm⁻¹ with the highest breakdown occurring at ca. 400 kV mm⁻¹. By integrating the D–E curve, the total input energy density at the maximum field is ca. 4 J cc⁻¹ with a corresponding energy loss of ca. 0.6 J cc⁻¹ (see the Supporting Information for plots) Therefore, the efficiency, at the highest field, of the blend is approximately 84%, in which the loss at high field can be attributed to conduction loss and not ferroelectricity. The calculated permittivity of the blend is found to be ca. 4, which is lower than what was calculated for the frequency domain measurements. This is a result of surface roughness of the film as the frequency domain measurements are taken over an area of 0.78 cm² versus the ball-bearing measurement on top of a sputtered electrode with an area of 0.07 cm². This indicates that morphology and uniformity of the film need to be improved which may lead to higher breakdown strengths and improved dielectric properties. Further studies will involve processing conditions, i.e., annealing temperature, casting technique, and so on to give uniformly smooth films.

In summary, these observations imply that the predicted octahedral structures are the realistic models to describe the experimentally synthesized Sn-ester-based polymer. These models exhibit not only a high-averaged dielectric constant ($\epsilon_{\text{avg}} = 4.7$) but also a wide calculated band gap ($E_g = 6.0$ eV). More importantly, there is a strong correlation between the predicted models and experimental data, with pDMTGlU exhibiting a dielectric constant of 6.22 with a band gap of 4.7 eV as well as some elucidation of the structural pattern of the polymer. In addition, it appears that the dielectric constant can be tuned depending upon what solution the film is cast from. The crystal size can be reduced through blending of a second homopolymer, which can disrupt chain packing without severely reducing the dielectric constant. These blends can then achieve breakdown strength up to 400 kV mm⁻¹, storing 4 J cc⁻¹ of energy. Improvement in pro-

cessing technique will be explored to give uniformly smooth films. As a result of these properties, Sn-ester-based polymers could be promising candidates for dielectric applications.

Experimental Section

Tetrahydrofuran (J.T. Baker, HPLC grade), glutaric acid (Acros Organics), and dimethyltin dichloride (TCl) were used as received. Into a round-bottom flask equipped with a magnetic stir bar 35.3167 g (267.3 mmol) of glutaric acid, 24.5259 g (613.1 mmol) of NaOH, and 350 mL of H₂O is added. To an Erlenmeyer flask 57.6832 g (262.6 mmol) of dimethyltin dichloride and 390 mL of THF is added. The dimethyltin dichloride solution is then added to the rapidly stirred diacid solution. After stirring for a minute, the reaction solution is quenched with aqueous NH₄Cl, the solid is then filtered, washed with 100 mL portions of THF and H₂O, and dried in vacuo to yield poly(dimethyltin glutarate) (51.5713 g, 70%) (see the Supporting Information for complete tabulation of characterization data).

Fourier transform infrared (FTIR) spectra were collected using a Nicolet Magna 560 FTIR spectrometer (resolution 0.35 cm⁻¹) and are reported in wavenumbers (cm⁻¹). The spectrum was obtained from a KBr pellet containing the title compound. Solution ¹H NMR (500 MHz) was performed using a Bruker DMX500 high-resolution digital NMR spectrometer. Thermogravimetric analysis (TGA) was performed using a TA instruments TGA Q500 with a heating rate of 10 °C min⁻¹ under N₂ atmosphere. Differential Scanning Calorimetry (DSC) was performed on a TA instruments DSC Q series with a first heating cycle rate of 40 °C min⁻¹, a cooling cycle of 40 °C min⁻¹ and a second heating cycle of 10 °C min⁻¹. Dielectric data were collected using an IMASS time domain dielectric spectrometer (TDDS) with measurements done in an air circulating oven at constant temperature. X-ray diffraction (XRD) data were collected on powdered samples using a Bruker D2 Phaser with a Cu-K α ($\lambda = 1.54184$ Å) radiation source. The polarization measurement was conducted with a modified Sawyer-Tower circuit, employing a Trek Model 10/40 10 kV high-voltage amplifier and an OPA541 operational amplifier-based current integrator. From the DE loop, the polarization, dielectric breakdown strength, total energy storage density, loss, relative permittivity, and discharge efficiency are derived. Stainless steel shim stocks (diameter: 2", thickness: 0.01", and ASTM A666 stainless steel) were procured from McMaster Carr. Quartz slides (3" × 1" × 1 mm) were procured from Ted Pella, Inc.

Supporting Information

Supporting Information is available from the Wiley Online Library or from the author.

Acknowledgements

This work was supported by a Multi-University Research Initiative (MURI) grant from the Office of Naval Research, under award number N00014-10-0944. The authors thank JoAnne Ronzello for performing all dielectric measurements, Maximilian Amsler and Stefan Goedecker for making available the minima hopping method code, and Zhe Qiang and Dr. Bryan Vogt for performing ellipsometry.

Received: September 9, 2014

Revised: October 15, 2014

Published online: November 25, 2014

[1] a) P. M. Hergenrother, *High Perform. Polym.* **2003**, *15*, 3; b) V. K. Thakur, M. R. Kessler, in *Advance Energy Materials*, Vol. 1 (Eds: A. Tiwari, S. Valyukh), Scrivener Publishing, Beverly, MA, USA

- 2014, Ch. 5; c) Y.-G. Ha, K. Everaerts, M. C. Hersam, T. J. Marks, *Acc. Chem. Res.*, **2014**, 47(4), 1019; d) T. Diekmann, U. Hilleringmann, in *Physical and Chemical Aspects of Organic Electronics*, Vol. 1 (Ed: C. Wöll), Wiley-VCH, Weinheim, Germany **2009**, Ch. 18; e) G. M. Rebeiz, in *RF MEMS: Theory, Design, and Technology*, Wiley, Hoboken, NJ, USA **2003**; f) N. Camaioni, R. Po, *J. Phys. Chem. Lett.*, **2013**, 4, 1821.
- [2] a) C. C. Wang, G. Pilania, S. A. Boggs, S. Kumar, C. Breneman, R. Ramprasad, *Polymer* **2014**, 55, 979; b) V. Sharma, C. C. Wang, R. G. Lorenzini, R. Ma, Q. Zhu, D. W. Sinkovits, G. Pilania, A. R. Oganov, S. Kumar, G. A. Sotzing, S. A. Boggs, R. Ramprasad, *Nat. Commun.* **2014**, 5, 4845.
- [3] Y. Ohki, N. Fuse, T. Arai, 2010 Annual Report Conference on Electrical Insulation and Dielectric Phenomena, West Lafayette, IN **2005**, pp. 1–4.
- [4] a) C.-G. Duan, W. N. Mei, J. R. Hardy, S. Ducharme, J. Choi, P. A. Dowben, *Europhys. Lett.* **2003**, 61, 81; b) B. Chu, X. Zhou, K. Ren, B. Neese, M. Lin, Q. Wang, F. Bauer, Q. M. Zhang, *Science* **2006**, 313, 334.
- [5] J. A. Chilton, *Plastics for Electronics*, (Ed. M. Goosey), Springer, New York **1999**, pp. 243–291.
- [6] X. Zhou, B. Chu, B. Neese, M. Lin, Q. M. Zhang, *IEEE Trans. Dielectr. Electr. Insul.* **2007**, 14, 1133.
- [7] a) X. Hao, *Adv. Dielectrics* **2013**, 3, 1330001; b) J. Y. Li, L. Zhang, S. Ducharme, *Appl. Phys. Lett.* **2007**, 90, 132901; c) D. Q. Tan, Q. Chen, P. Irwin, Y. U. Wang, *IEEE Trans. Ultrason. Ferroelectr. Freq. Control.* **2013**, 60, 1619; d) Z. M. Dang, J.-K. Yuan, S.-H. Yao, R.-J. Liao, *Adv. Mater.* **2013**, 25, 6334.
- [8] G. Pilania, C. C. Wang, K. Wu, N. Sukumar, C. Breneman, G. Sotzing, R. Ramprasad, *J. Chem. Info. Model.* **2013**, 53, 879.
- [9] a) A. S. Abd-El-Aziz, C. E. Carraher, C. U. Pittman, M. Zeldin, *Macromolecules Containing Metal and Metal-Like Elements, Group IVA Polymers*, Vol. 4, Wiley-Interscience, Hoboken, NJ, USA **2005**, p. 264; b) R. V. Subramanian, K. N. Somasekharan, *J. Macromol. Sci., Chem.* **1981**, A16, 73; c) A. ur-Rehman, M. Hussain, A. Rauf, A. A. Tahir, S. Ali, *J. Inorg. Organomet. Polym.* **2012**, 22, 699; d) I. Manners, *Angew. Chem Int. Ed. Engl.* **1996**, 35, 1602.
- [10] a) C. E. Carraher Jr., M. R. Roner, *Materials* **2009**, 2, 1558; b) C. E. Carraher Jr., D. O. Winter, *Die Makromol. Chem.* **1972**, 152, 55; c) C. E. Carraher Jr., R. L. Dammeier, *Die Makromol. Chem.* **1970**, 135, 107; d) S. D. Bhagat, J. Chatterjee, B. Chen, A. E. Stiegman, *Macromolecules* **2012**, 45, 1174.
- [11] a) S. Chisca, V.-E. Musteata, I. Sava, M. Bruma, *Eur. Polym. J.* **2011**, 47, 1186; b) M.-D. Damaceanu, V.-E. Musteata, M. Cristea, M. Bruma, *Eur. Polym. J.* **2010**, 46, 1049.
- [12] a) A. F. Baldwin, R. Ma, C. C. Wang, R. Ramprasad, G. A. Sotzing, *J. Appl. Polym. Sci.* **2013**, 22, 699; b) R. Ma, A. F. Baldwin, C. C. Wang, I. Offenbach, M. Cakmak, R. Ramprasad, G. A. Sotzing, *ACS Appl. Mater. Interfaces* **2014**, 6, 10443.
- [13] a) P. Hohenberg, W. Kohn, *Phys. Rev.* **1964**, 136, B864; b) W. Kohn, L. Sham, *Phys. Rev.* **1965**, 140, A1133.
- [14] a) G. Kresse, J. Hafner, *Phys. Rev. B* **1993**, 47, 558; b) G. Kresse, *Ph.D. thesis, Technische Universität Wien, Austria* **1993**; c) G. Kresse, J. Furthmüller, *J. Comput. Mater. Sci.* **1996**, 6, 15; d) G. Kresse, J. Furthmüller, *Phys. Rev. B* **1996**, 54, 11169.
- [15] J. P. Perdew, K. Burke, M. Ernzerhof, *Phys. Rev. Lett.* **1996**, 77, 3865.
- [16] a) S. Goedecker, *J. Chem. Phys.* **2004**, 120, 9911; b) M. Amsler, S. Goedecker, *J. Chem. Phys.* **2010**, 133, 224104.
- [17] S. Baroni, S. de Gironcoli, A. Dal Corso, *Rev. Mod. Phys.* **2001**, 73, 515.
- [18] J. Heyd, G. E. Scuseria, M. Ernzerhof, *J. Chem. Phys.* **2006**, 124, 219906.
- [19] S. Grimme, *J. Comp. Chem.* **2006**, 27, 1787.
- [20] X. Xiao, X. Han, Z. Mei, D. Zhu, K. Shao, J. Liang, *J. Organomet. Chem.* **2013**, 729, 28.
- [21] C. E. Carraher Jr., *Die Angew. Makromol. Chem.* **1973**, 31, 115.
- [22] a) A. G. Davies, *Organotin Chemistry*, Wiley-VCH, Weinheim, Germany **2004**, p. 205; b) J. Hussain, M. Hussain, V. U. Ahmad, A. Al-Harras, A. Badshah, *Org. Commun.* **2012**, 5, 18; c) M. Ashfaq, M. M. Ahmed, S. Shaheen, H. Oku, K. Mehmood, A. Khan, S. B. Niazi, T. M. Ansari, A. Jabbar, M. I. Khan, *Inorg. Chem. Commun.* **2011**, 14, 5.
- [23] a) G. Plazzogna, V. Peruzzo, G. Tagliavini, *J. Organomet. Chem.* **1969**, 16, 500; b) V. Peruzzo, G. Plazzogna, G. Tagliavini, *Organomet. Chem.* **1969**, 18, 89; c) V. Peruzzo, G. Plazzogna, G. Tagliavini, *Organomet. Chem.* **1970**, 24, 347; d) V. Peruzzo, G. Plazzogna, G. Tagliavini, *Organomet. Chem.* **1972**, 40, 129.